Characterizing Ultra-Low Intermodulation Distortion in RF Switches for Sub-6GHz Applications

M. Ben-Sassi, H. Saleh, F. Drillet, O. Sow, I. Lahbib, Greg U'ren, C. Hallepee, D. Passererieux, G. Neveux, Denis Barataud

Characterizing Ultra-Low Intermodulation Distortion in RF Switches for Sub-6GHz Applications.

M. Ben-Sassi[#1], H. Saleh[#2], F. Drillet[#3], O. Sow[#4], I. Lahbib[#5], Greg D. U'Ren[#6], C. Hallepee[*7], D. Passererieux[*8], G. Neveux[*9], D. Barataud[*10]

[*]XLIM Laboratory, UMR CNRS n°7252, University of Limoges, Faculté des Sciences et Techniques, Campus La Borie
[*]X-FAB, France
{[1]Marwen.Ben-Sassi, [2]Hassan.Saleh, [3]Frederic.Drillet, [4]Ousmane.Sow, [5]Imene.Lahbib, [6]Gregory.Uren}@xfab.com,
{[7]clement.hallepee, [8]damien.passerieux, [9]guillaume.neveux, [10]denis.barataud}@xlim.fr

***Abstract* — This paper presents apparatus and measurement results for ultra-low third-order Inter-Modulation-Distortion (IMD3) products of RF switches, with power levels below -100 dBm. Two setups are developed and calibrated for IMD3 measurements at 2.64 GHz and 5.4 GHz, respectively. The duplexers, the core components of the setups, are configured with a passband and stopband architecture to ensure a 50 Ω out-of-band environment, making the measurements independent of phase variations. With the stopband filter, the duplexers filter out the two high-power signal tones to prevent receiver compression, while allowing IMD3 signals to pass with low attenuation, enabling measurements with a high vertical dynamic range. SP6T RF switches from X-FAB foundry were characterized using the presented apparatus, achieving IMD3 measurements with power levels below -100 dBm.**

***Keywords* — Inter-Modulation-Distortion, RF linearity, RF switch, IMD measurement, Stopband filter.**

I. Introduction

New mobile communication generations are continuously advancing in terms of data rates, the number of available frequency bands, and absolute power levels. Data rate enhancements are achieved through various techniques, including inter-operation Frequency and Time Division Duplexing (FDD and TDD), high-order modulation schemes, Multiple-Inputs Multiple-Outputs (MIMO), adaptive antenna systems, and Carrier Aggregation (CA) [1], [2]. CA boosts the available data rate by enabling transmission and reception on multiple frequencies: multiple receive bands are available, and the incoming signal is routed from the antenna to the appropriate receive path through an antenna diversity switch (Fig. 1).

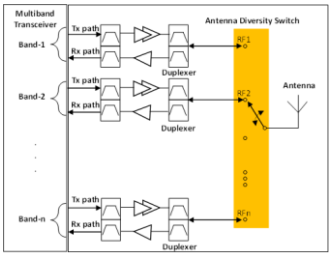

Fig. 1. Block diagram of a cellular RF.

The use of multiple frequency bands simultaneously for uplink and downlink in the switch generates unwanted intermodulation products. If the switch used for band selection lacks sufficient linearity, undesired intermodulation products may fall within another receive frequency band and interfere with the received signal (Fig. 2). Therefore, the out-of-band blocking characteristic becomes a crucial linearity specification for switches [3], [4], [5]. This characteristic can be quantified by the Third-order Inter-Modulation-Distortion (IMD3).

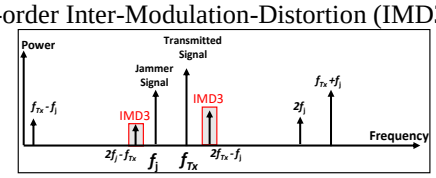

Fig. 2. Block diagram of a cellular RF.

Measurement of IMD3 power levels in RF switches presents a challenge due to their extremely low power levels compared to those of the main signals. In [6], the measurement setup addressed Wideband Code Division Multiple Access (WCDMA) bands below 2 GHz and made use of a duplexer with a highly reflective impedance at IMD3 frequencies. The use of a phase shifter was essential to explore the various possible IMD3 scenarios with a 20-dB difference between their minimum and maximum levels. The setups utilized in [7] allowed IMD3 characterization at Long Term Evolution (LTE) bands between 800 MHz and 2.5 GHz using a setup similar to that in [1]. Other close set-ups to characterize Passive Intermodulation Measurements (PIM) have been developed [8] below 5 GHz and at K-/Ka-bands but they are not dedicated to measurements of active SPxT switches. In our previous work [8], we presented a comparison between measurements and Harmonic Balance Simulations of IMD3 from RF switches at frequencies below 2 GHz. Duplexers were configured with two passband filters, similar to [6] and [7]. In this work, we introduce an IMD3 characterization setup at 2.64 GHz and 5.4 GHz. To the best of our knowledge, this is the first time that IMD3 measurements of switches have been presented at a frequency as high as 5.4 GHz. To achieve the required measurement sensitivity of -110 dBm and minimize IMD3's dependency on phase angle, the proposed setups utilize stopband and bandpass filters in the duplexer instead of two bandpass filters to avoid out-of-band impedance mismatch at the Rx port. Duplexers were selected to have low insertion losses at Tx passbands and high rejection at stopbands. This paper demonstrates that the variation in IMD3 levels with phase

shift is insignificant when the duplexer impedance at IMD3 frequencies is close to 50 Ω, rendering the use of a phase shifter in that case unnecessary. The next section describes the block diagrams of the two characterization setups we developed, enabling the measurement of ultra-low IMD3 power levels at 2.64 GHz and 5.4 GHz, respectively. Section III presents the S-parameters measurements of two selected duplexers for IMD3 measurements. IMD3 measurement results from RF switch demonstrators and their sensitivity to phase variation are presented in sections V and VI, respectively. The work concludes in section VII.

II. Experimental IMD3 Test Bench

The general block diagram of the two measurement setups for measurement of RF switches is presented in Fig. 3.

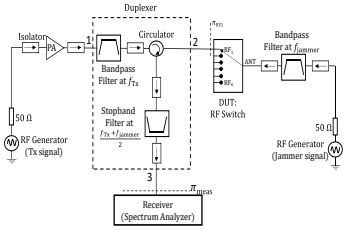

Fig. 3. General block diagram of the 2 IMD3 setups @ 2.64 GHz & 5.4 GHz.

The photograph of the experimental measurement setup at 2.64 GHz for measurement of RF switches is presented in Fig. 4.

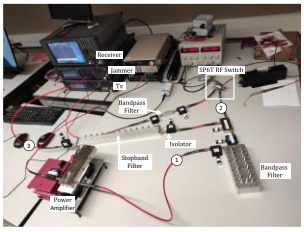

Fig. 4. Photograph of the IMD3 measurement setup at 2.64 GHz. Duplexer inputs and outputs are indicated by the labels 1, 2 and 3, same as Fig. 3.

Two RF sources drive the RF switch with two signals f_{Tx} (transmit port) and f_{jammer} (antenna port) with two different power levels P_{Tx} and P_{jammer} respectively, with P_{Tx} greater than P_{jammer}. The values of the fundamental frequencies and the associated power ranges are summarized in Table 1.

Table 1. Frequencies and power specifications.

Setup	Frequencies (GHz)	Power sweep (dBm)
IMD3 (2.64 GHz)	$f_{Tx} = 2.54$	$P_{Tx} \in [0; 32]$
	$f_{jammer} = 2.44$	$P_{jammer} \in [-26; 0]$
IMD3 (5.4 GHz)	$f_{Tx} = 5.3$	$P_{Tx} \in [0; 32]$
	$f_{jammer} = 5.2$	$P_{jammer} \in [-26; 0]$

A wideband 2-6 GHz Power Amplifier (PA) with a high linearity and a 50-dB gain was used throughout the experiment. The PA remains the same for the two setups. However, the narrowband isolators, filters and circulators are specific for each of the setups and are carefully chosen to operate in two distinct frequency bands, 2.64 GHz and 5.4 GHz, respectively. Their specifications are described in the following section. A pivotal aspect of this architecture is the utilization of a receiver with high sensitivity and a low noise floor, enabling the measurement of the low-power IMD3 signals. To achieve this, a spectrum analyzer (Keysight MXA) was employed, allowing measurements with different narrowband windows with varying settings such as span, Resolution Bandwidth (RBW), Video Bandwidth (VBW), Attenuation and FFT-Sweep. This multipronged configuration scheme enhances measurement accuracy. Table 2 displays the two IMD3 frequencies of interest. The absolute power levels at f_{1_IMD3} and f_{2_IMD3} are measured in the receiver plane π_{meas}.

Table 2. IMD3 frequencies of interest.

Setup	IMD3 frequencies Definitions	IMD3 frequencies and Values (GHz)
IMD3 (2.64 GHz)	$2 \times f_{jammer} - f_{Tx}$	$f_{1\_IMD3} = 2.34$
	$2 \times f_{Tx} - f_{jammer}$	$f_{2\_IMD3} = 2.64$
IMD3 (5.4 GHz)	$2 \times f_{jammer} - f_{Tx}$	$f_{1\_IMD3} = 5.1$
	$2 \times f_{Tx} - f_{jammer}$	$f_{2\_IMD3} = 5.4$

To obtain calibrated IMD3 power levels at the DUT output plane π_{RF1}, a power calibration procedure was conducted. Initially, S-parameters of the duplexers were measured at all frequencies of interest, allowing the determination of insertion loss coefficients. Subsequently, the input signals, Tx and jammer, were measured in the DUT planes using a power sensor to ensure they met the required levels. Finally, the IMD3 signal powers were measured in the receiver plane π_{meas} and calibrated using the determined insertion loss coefficients.

III. Duplexers

The schematic of the utilized duplexers is detailed in Fig 3 (dotted rectangle). Each of the duplexers consists of a bandpass filter in the Tx path and a stopband filter in the Rx path to insure a 50 Ω impedance at Rx port. While the duplexers share similar architectures in both setups, they operate at different frequency bands. The bandpass filter is centered at f_{Tx} and is narrowband, effectively filtering out any spurious or harmonic component of the Tx signal. The stopband filter is centered at $\frac{f_{Tx}+f_{jammer}}{2}$ to eliminate the Tx and jammer signals at the receiver, preventing compression and maintaining a good dynamic range for IMD3 measurement. Additionally, the dual-junction circulator ensures a high isolation of 40 dB between the jammer signal and the Rx port. The three-port S-parameters measurements of the two duplexers are presented in the Fig. 5 (a) and Fig. 5 (b), respectively.

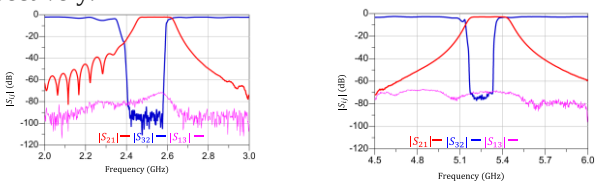

(a) (b)

Fig. 5. $|S_{21}(f)|$, $|S_{32}(f)|$ and $|S_{13}(f)|$ of the duplexer for the 2.64 GHz apparatus (a) and for the 5.4 GHz apparatus (b).

IV. Device Under Test (DUT): RF Switches.

The 130nm RF-SOI platform from X-FAB foundry was chosen for designing and manufacturing the two Single Pole Six Throws (SP6T) RF switches. They feature symmetrical reflective architectures that utilize series and shunt branches in a partially depleted process. The two SP6T circuits operate in the sub-3GHz and sub-6GHz frequency ranges, respectively. Fig. 6 (a) and 6 (b) display photographs of both SP6T switch demonstrators.

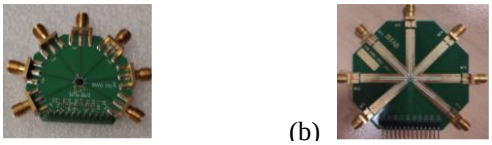

(a) (b)

Fig. 6. X-FAB switch demonstrator operates in sub-3GHz (a), X-FAB switch demonstrator operates in sub-6GHz (b).

V. IMD3 Measurement Results.

The spectrum analyzer configuration, including span, number of points, Resolution Bandwidth (RBW), and FFT Sweep, remains consistent for both measured IMD3 power levels and is detailed in Table 3

Table 2. Spectrum Analyzer Configuration.

Center Frequency	Span	Points	Resolution Bandwidth	Sweep (FFT)
f_{1_IMD3}	1 MHz	1001	1Hz	9.73s
f_{2_IMD3}				

Fig. 7 (a) and 7 (b) display the measured IMD3 signals from the two SP6T switches, as presented in the previous section, operating within the two operation frequency bands. The transmitted signal power level is 26 dBm, while the jammer signal power level is -15 dBm. It's worth noting that these two signals are not present in the receive measurement plane due to their effective filtration using the stopband filter. Unlike a passband filter, the use of a stopband filter enables the measurement of power levels at both frequency components of IMD3 products. In Fig. 7 (a), the absolute power level of IMD3 at 2.64 GHz is -109 dBm, while the IMD3 at 2.34 GHz registers below -135 dBm, which corresponds to the receiver's noise floor. Similarly, in Fig. 7 (b), the setup at 5.4 GHz facilitates the measurement of absolute power levels for IMD3 products at 5.1 GHz and 5.4 GHz, yielding values of -120 dBm and -81 dBm, respectively.

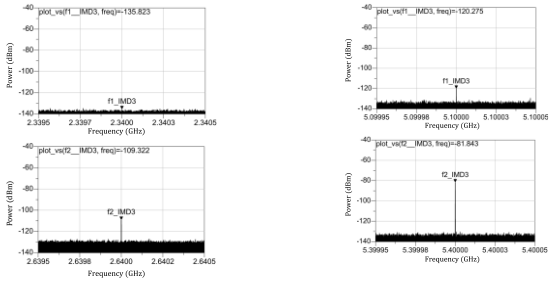

(a) (b)

Fig. 7. Measured and calibrated absolute power levels at the two IMD3 frequencies for the setup at 2.64 GHz (a), and at 5.4GHz (b).

Additionally, by employing the developed test bench at 5.4 GHz, we measured IMD3 products as the power levels at the two fundamental frequencies were swept.

Fig. 8 (a) and 8 (b) illustrate the measured absolute power levels at f_{1_IMD3}=5.1 GHz and f_{2_IMD3}=5.4 GHz, respectively. The absolute power at f_{Tx}=5.3 GHz remains fixed at 26 dBm, while the absolute power at f_{jammer}=5.2 GHz is swept within the range specified in Table I, between -26 and 0 dBm.

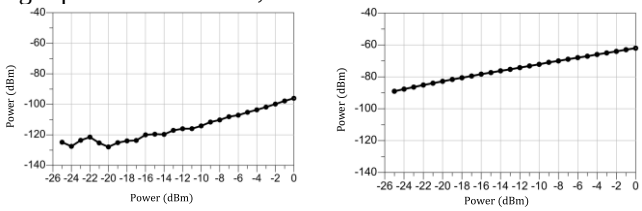

(a) (b)

Fig. 8. Calibrated measured IMD3 power levels at: f_{1_IMD3}=5.1 GHz (a) and f_{1_IMD3}=5.4 GHz (b) for P_{Tx}=26 dBm and P_{jammer} swept between -26 dBm to 0 dBm.

Increasing the input power P_{jammer}, as shown in the Fig. 8 has an impact on the IMD3 measurement results, even at 5.1 GHz when the measured power is extremely low. In Fig. 8 (b), the slope of the higher intermodulation frequency f_{2_IMD3} curve is 1 dB/dB, confirming the linear behaviour of the switch in that scenario.

Fig. 9 (a) and 9 (b) present the measured power levels at f_{1_IMD3}=5.1 GHz and f_{2_IMD3} =5.4 GHz, respectively, while the power of f_{Tx} =5.3 GHz is swept from 20 dBm to 30 dBm, and the f_{iammer} signal at the antenna port remains constant at -15 dBm.

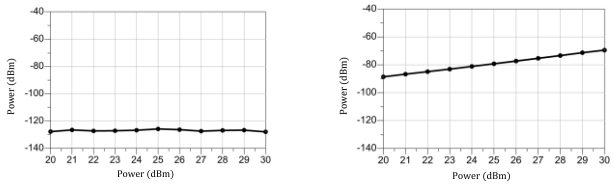

(a) (b)

Fig. 8. Calibrated measured IMD3 power levels at: f_{1_IMD3}=5.1 GHz (a) and f_{1_IMD3}=5.4 GHz (b) for P_{jammer} =-15 dBm and P_{Tx} swept between 20 dBm to 30 dBm.

As theoretically expected, in Fig. 8 (b), the measured power levels at f_{2_IMD3}=5.4 GHz are adversely affected by the increase in input power P_{Tx}. The slope of the higher intermodulation frequency f_{2_IMD3} curve is 2 dB/dB, indicating a slight non-linear behavior of the switch.

VI. Sensitivity to Phase Variation.

To evaluate the influence of signal phase variation on the IMD3 products, similar to the approach in [6] and [10], a phase shifter has been incorporated into the 2.64 GHz measurement setup while measuring the sub-3GHz SP6T RF switch, as depicted in Fig. 9.

Fig. 10 illustrates the calibrated measured power levels of the IMD3 signal at 2.64 GHz, at the RF output port of the SP6T, as a function of phase angle on the Tx signal.

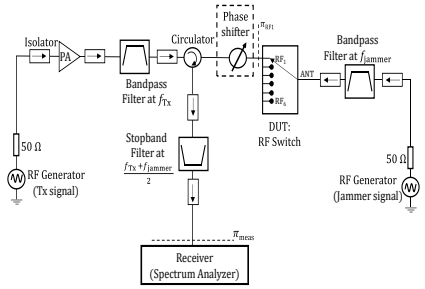

Fig. 9. IMD3 measurement setup at 2.64 GHz including a phase shifter.

The variation in IMD3 power levels remains within a 3 dB for a wide phase variation spanning [0°; 180°] of the phase shifter. This contrasts with other works [6], where a variation on the order of 20 dB has been reported with a duplexer architecture employing two bandpass filters.

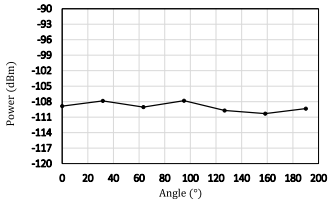

Fig. 9. IMD3 measurement setup at 2.64 GHz including a phase shifter.

To elucidate the source of IMD3 sensitivity to phase variation, impedance parameters at the three duplexer ports were measured. Using the S-parameters, the corresponding real and imaginary parts of the impedances were calculated and are depicted in Fig. 10.

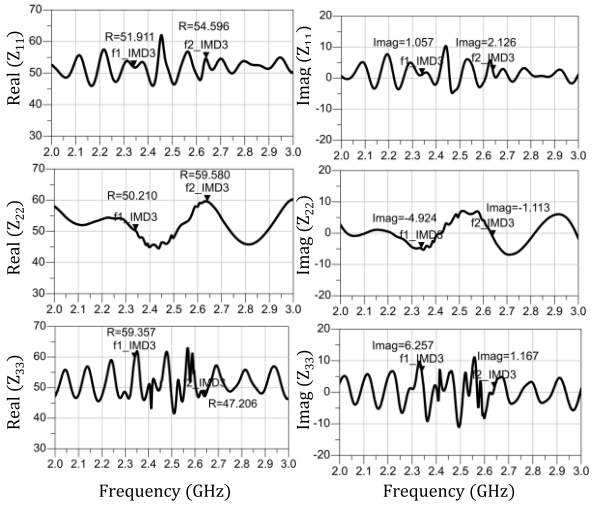

Fig. 10. Real & Imaginary Parts of $Z_{11}(f)$, $Z_{22}(f)$ and $Z_{33}(f)$ from the 2.64 GHz duplexer, Markers indicate impedance values at f_{1_IMD3} and f_{2_IMD3}.

The presented impedance values exhibit stability as a function of frequency, hovering around 50 Ω (real part) and around 0 Ω (imaginary part). This nearly 50 Ω environment within the band of interest is attributed to the use of a stopband filter to block the Tx and jammer signals. Consequently, the IMD3 products become nearly independent of potential signal reflections at the duplexer input ports. Such a condition isn't met with duplexers using 2 bandpass filters [6] leading to significant IMD3 variations power with respect to the phase angle. This result underscores a key novelty of this work and confirms the advantages of using a stopband filter within the duplexer.

VII. Conclusion

This paper introduces two apparatus for measuring intermodulation distortion (IMD3) in RF switches, operating at 2.64 GHz and 5.4 GHz. A significant innovation in this work lies in the high-frequency capabilities and the establishment of a 50 Ω environment through the use of a stopband filter. Furthermore, the measurement setups offer a notable vertical dynamic range. A calibration procedure, based on S-parameter measurements, has been successfully implemented.

The developed IMD3 setups enable the measurement of ultra-low power levels, reaching as low as -120 dBm. To the best of our knowledge, this represents the state of the art for these applications. Based on our findings, the utilization of a phase shifter in IMD3 experiments is not mandatory when the duplexer architecture incorporates a stopband filter on the receiver side, as the IMD3 products exhibit minimal dependency on the phase angle.

References

[1] 3GPP, "3rd Generation Partnership Project; Technical Specification Group Services and System Aspects; IP Multimedia Subsystem (IMS) based Packet Switch Streaming (PSS) and Multimedia Broadcast/Multicast (MBMS) User Service; Protocols," Release 17.0.0, Dec. 2021. Available: https://www.3gpp.org/ftp/Specs/archive/26_series/26.237/.

[2] V. N. K. Malladi and M. Miller, "A 48 dBm peak power RF switch in SOI process for 5G mMIMO applications," *2019 IEEE 19th Topical Meeting on Silicon Monolithic Integrated Circuits in RF Systems (SiRF)*, Orlando, FL, USA, 2019, pp. 1-3, doi: 10.1109/SIRF.2019.8709096.

[3] A. Tombak, et al., "Design of High-Order Switches for Multimode Applications on a Silicon-on-Insulator Technology," in *IEEE Transactions on Microwave Theory and Techniques*, vol. 61, no. 10, pp. 3639-3649, Oct. 2013, doi: 10.1109/TMTT.2013.2277989

[4] T. G. McKay, P. R. Verma, S. Zhang, J. S. Wong and J. Brunner, "Switch branch in trap-rich RFSOI with 84 dBm off-state IP3," *2015 IEEE SOI-3D-Subthreshold Microelectronics Technology Unified Conference (S3S)*, Rohnert Park, CA, USA, 2015, pp. 1-3, doi: 10.1109/S3S.2015.7333531

[5] C. Li, O. Elaassar, N. Satish, A. Kumar, N. Cahoon and G. Rebeiz, "5G mm-Wave SPDT Switch IMDn Investigation," *2019 IEEE MTT-S International Microwave Conference on Hardware and Systems for 5G and Beyond (IMC-5G)*, Atlanta, GA, USA, 2019, pp. 1-3, doi: 10.1109/IMC-5G47857.2019.9160367

[6] T. Ranta, J. Ella and H. Pohjonen, "Antenna switch linearity requirements for GSM/WCDMA mobile phone front-ends," *The European Conference on Wireless Technology, 2005.*, Paris, France, 2005, pp. 23-26, doi: 10.1109/ECWT.2005.1617645.

[7] Infineon Technologies. *Wideband SP3T RF Switch for RF diversity or RF band selection applications Revision 1.0* (2016). [Online]. Available: https://www.farnell.com/datasheets/2355019.pdf.

[8] D. Smacchia *et al*., "Advanced Compact Setups for Passive Intermodulation Measurements of Satellite Hardware," in *IEEE Transactions on Microwave Theory and Techniques*, vol. 66, no. 2, pp. 700-710, Feb. 2018, doi: 10.1109/TMTT.2017.2783383.

[9] M. Ben-Sassi et al., "Intermodulation Products of a CMOS SP6T Antenna Switch: Results Comparison Between an Experimental Test-Bench and a Corresponding Simulated Virtual Test-Bench," 2021 16th European Microwave Integrated Circuits Conference (EuMIC), London, United Kingdom, 2022, pp. 9-12, doi: 10.23919/EuMIC50153.2022.9783860.

[10] S. Moss, E. Veeramani and J. A. S. Jerome, "Passive Intermodulation (PIM) Test and Measurement," *2020 IEEE 29th North Atlantic Test Workshop (NATW)*, Albany, NY, USA, 2020, pp. 1-3, doi: 10.1109/NATW49237.2020.9153075.